

$[11\bar{3}]$ -directed open orbits supported by the model CU VI traced out in the compilation of the data for Fig. 10. This orbit lies just inside the shaded region at a relative $k_z=0.15$ and at an angle 12° between the field and $[1\bar{1}0]$ axis.

Based on the above arguments, we find that Roaf's phenomenological FS model CU VI is in good accord with our galvanomagnetic measurements with respect to Hall constant values and angular extent of various one- and two-dimensional regions.

Core-Polarization Contribution to the Knight Shift in Beryllium Metal*

WEI-MEI SHYU, G. D. GASPARI,[†] AND T. P. DAS

Department of Physics, University of California, Riverside, California

(Received 1 June 1965)

Direct and core-polarization contributions to the Knight shift in beryllium metal were calculated at a number of symmetry points near the Fermi surface. The direct contribution was evaluated using wave functions for the conduction electrons by the orthogonalized-plane-wave method. The contribution of the core electrons was determined using the moment-perturbation (MP) method developed in an earlier paper. The accuracy of the MP method was rechecked by calculating the core contribution to the hyperfine coupling constant in the 3P_2 state of the beryllium atom. Good agreement was obtained with the result of an earlier self-consistent-field calculation by Goodings. For the Γ_4^- level, the direct and core contributions to the Knight shift are 0.01536 and 0.00258%, respectively. For the two degenerate levels of H_1 , the direct contributions both vanish while the core-polarization contributions are -0.00061 and -0.00001% . These results lead to the conclusion that core-polarization effects alone can not explain the near-vanishing Knight shift observed experimentally in beryllium metal. Some other contributions such as those from various orbital mechanisms would therefore have to be considered.

I. INTRODUCTION

A NUMBER of recent papers¹⁻⁴ have dealt with the theory of the Knight shift in beryllium metal. Earlier measurement by Knight^{1,5} showed that the Knight shift was less than 0.002%; that is, essentially zero within experimental error. The theoretical investigations, on the other hand, while they differ quantitatively in their predictions, all lead to finite values of the Knight shift which are beyond the range of experimental error.

Since beryllium is a light metal with only one core state, one would expect an analysis of the Knight shift to be relatively easier compared to heavier metals. In heavier metals the spin-orbit and other relativistic effects and the problem of orthogonality to core states lead to complications in the calculation of the wave functions for conduction electrons. It is therefore important to understand the reasons for the disagreement between theoretical and experimental results for Be.

The first source that comes to mind is possible inaccuracies in the wave function employed to make the theoretical estimates of Knight shift in earlier papers. Wood and Milford³ employed augmented plane-wavefunctions based on earlier calculations by Jacques.⁶ They assumed a spherical Fermi surface and found that the Knight shift is appreciable. A spherical Fermi surface was also assumed by Pomerantz and Das² who used an orthogonalized-plane-wave (OPW) calculation and found the Knight shift to be substantial. Townes, Herring, and Knight¹ obtained their Knight shift result from Herring and Hill's OPW calculation.⁷ Herring and Hill determined the energy levels at a number of points and lines in \mathbf{k} space but did not include many OPW functions in their calculation owing to the lack of computing facilities at the time. The most recent calculations on the band structure and Fermi surface of Be metal are due to Loucks and Cutler⁸ and Loucks,⁹ who made a careful study of the potential to reach a certain degree of self-consistency and obtained energy levels at a number of points using fairly high order secular equations. They found quite good agreement with the available de Haas-van Alphen data¹⁰ and soft x-ray spectro-

* Supported by the National Science Foundation.

[†] Present address: Department of Physics, University of Rochester, Rochester, New York.

¹ C. H. Townes, C. Herring, and W. D. Knight, *Phys. Rev.* **77**, 852 (1950).

² M. Pomerantz and T. P. Das, *Phys. Rev.* **119**, 70 (1960).

³ V. E. Wood and F. J. Milford, *J. Phys. Chem. Solids* **23**, 160 (1962).

⁴ W. Schneider, L. Jansen, and L. Etienne-Amberg, *Physica (Netherlands)*, **30**, 84 (1964).

⁵ W. D. Knight, *Solid State Physics*, edited by F. Seitz and D. Turnbull (Academic Press Inc., New York, 1956), Vol. 2.

⁶ R. Jacques, *Cahiers de Phys.* **70**, 1 (1956); **71-72**, 23 (1956); **75-76**, 17 (1956).

⁷ C. Herring and A. G. Hill, *Phys. Rev.* **58**, 132 (1940).

⁸ T. L. Loucks and P. H. Cutler, *Phys. Rev.* **133**, A819 (1964).

⁹ T. L. Loucks, *Phys. Rev.* **134**, A1618 (1964).

¹⁰ B. R. Watts, *Phys. Letters* **3**, 284 (1963).

scopic data.^{11,12} One would therefore expect wave functions obtained from their potential to be reasonably accurate and reliable. We have computed the energies and wave functions at a few points in \mathbf{k} space using their potential and found the convergence in both energies and wave functions to be very good. The Knight shift at the Γ point where a substantial part of the Fermi surface is located came out of our calculation to be appreciable. One therefore has to look for causes other than error in the direct Knight shift to explain the experimental data. One explanation that has been proposed by Sondheimer and Das¹³ is a Landau-type diamagnetic shielding. Sondheimer and Das have made a semi-quantitative estimate of the diamagnetic shielding using the effective-mass approximation and showed that it is possible to get a diamagnetic-shielding term comparable in magnitude to the direct Knight-shift term. In addition, one could also get an orbital contribution to the magnetic shielding which is analogous to the Lamb and Ramsey¹⁴ type of contribution in molecules and non-metals. Hebborn and Stephen¹⁵ have worked out elaborate expressions for Bloch electrons which incorporate the Landau and Lamb and Ramsey type contributions. However, these expressions are rather difficult to use for quantitative estimates. The other important mechanism which could contribute significantly to the Knight shift is the core-polarization effect which has been discussed by a number of authors.¹⁶⁻¹⁸ In the case of Be this effect would correspond to a contribution from the core $1s$ electrons due to their spin polarization by exchange interactions with the conduction electrons. In this paper, we have carried out a calculation of this core-polarization effect for Be metal using the moment-perturbation (MP) method developed in an earlier paper.¹⁷ It is found that the core polarization is in the wrong direction to remove the discrepancy between the computed direct contribution to the Knight shift and experiment.

In Sec. II we have used the MP method to compute the contribution from the core-polarization effect to the hyperfine constant for the 3P_2 term of the Be $1s^2 2s 2p$ state. Our result is very close to that from Goodings' unrestricted Hartree-Fock (UHF) calculation.¹⁹ The total hyperfine constant is found to be in good agreement with experiment.²⁰

¹¹ P. Fisher, R. S. Crisp, and S. E. Williams, *Optica Acta* **5**, 31 (1958).

¹² T. Sagawa, *Sci. Rept. Tohoku Univ. Ser. 45*, No. 4 (1961).

¹³ T. P. Das and E. H. Sondheimer, *Phil. Mag.* **5**, 529 (1960).

¹⁴ N. F. Ramsey, *Phys. Rev.* **78**, 699 (1950).

¹⁵ J. E. Hebborn and M. J. Stephen, *Proc. Phys. Soc. (London)* **80**, 991 (1962).

¹⁶ M. H. Cohen, D. A. Goodings, and V. Heine, *Proc. Phys. Soc. (London)* **73**, 811 (1959).

¹⁷ G. D. Gaspari, Wei-Mei Shyu, and T. P. Das, *Phys. Rev.* **134**, A852 (1964).

¹⁸ R. E. Watson and A. J. Freeman, *Phys. Rev.* **123**, 2027 (1961).

¹⁹ D. A. Goodings, *Phys. Rev.* **123**, 1706 (1961).

²⁰ A. Lurio and A. G. Blachman, *Bull. Am. Phys. Soc.* **6**, 142 (1961).

In Sec. III the wave-function calculation in Be metal is described. Convergence tests are carried out both for the energy and wave function.

In Sec. IV the core-polarization calculation is described and the significance of the results is discussed.

II. RESUMÉ OF THE MP METHOD AND APPLICATION TO THE TRIPLET P STATE (3P_2) OF THE Be ATOM

In an earlier paper,¹⁷ the theory of the MP method was developed and it was applied to study hyperfine interaction in the Li atom and Li metal. Actually, the Li atom is the least favorable case for a perturbation approach because of the small number of electrons involved. However, we found in the case of Li that both perturbation approaches, the MP¹⁷ as well as the EP¹⁶ (exchange-perturbation) method gave answers only about 15% different from the unrestricted Hartree-Fock approach of Sachs²¹ and Goodings.¹⁹ Since Be involves one more electron, we would expect the perturbation result to be even better and in closer agreement with the UHF method. To test this point and also to obtain a check on the perturbed wave function to be used subsequently for the core polarization calculation in the metal we have performed a MP calculation on the 3P_2 Be $1s^2 2s 2p$ state. The result of this calculation will be described in this section. For the sake of completeness we start with a brief resumé of the theory of the MP method.

Suppose we have an unperturbed system governed by the zero-order Schrödinger equation

$$H_0\Psi_0 = E_0\Psi_0. \quad (1)$$

We are interested here in the second-order change $E_{eN}^{(2)}$ in the energy of the system, due to its combined interaction with two first-order-perturbing Hamiltonians H_E and H_N . It can be shown¹⁷ that to first order in either H_E or H_N , the order of application of H_E and H_N is immaterial and $E_{eN}^{(2)}$ is given by either of the following two expressions.

$$E_{eN}^{(2)} = 2\langle\delta\Psi_E|H_N|\Psi_0\rangle, \quad (2)$$

$$E_{eN}^{(2)} = 2\langle\delta\Psi_N|H_E|\Psi_0\rangle, \quad (3)$$

where $\delta\Psi_E$ is the solution of the first-order equation

$$(H_0 - E_0)\delta\Psi_E = -(H_E - E_e)\Psi_0, \quad (4)$$

with

$$\langle\delta\Psi_E|\Psi_0\rangle = 0,$$

and

$$E_e = \langle\Psi_0|H_E|\Psi_0\rangle, \quad (5)$$

and $\delta\Psi_N$ is the solution of the equation

$$(H_0 - E_0)\delta\Psi_N = -(H_N - E_N)\Psi_0, \quad (6)$$

with

$$\langle\delta\Psi_N|\Psi_0\rangle = 0$$

²¹L. M. Sachs, *Phys. Rev.* **117**, 1504 (1960).

and

$$E_N = \langle \Psi_0 | H_N | \Psi_0 \rangle. \quad (7)$$

The fact that $E_{eN}^{(2)}$ can be obtained from either Eq. (2) or Eq. (3) leads to two different approaches for obtaining $E_{eN}^{(2)}$. In the problem at hand H_N describes the Fermi contact interaction of the nuclear moment with the core electrons and H_E , the exchange perturbation potential produced by the valence electrons at the site of the core-electron. For the exchange-perturbation method¹⁶ one determines $\delta\Psi_E$ by solving Eq. (4) and obtains $E_{eN}^{(2)}$ using Eq. (2). On the other hand, for the second approach or the moment perturbation method¹⁷ $\delta\Psi_N$ is determined by solving Eq. (6) and $E_{eN}^{(2)}$ is subsequently obtained from Eq. (3). In principle, these two methods are entirely equivalent. However, the MP method has some practical computational advantage and is more flexible in its application to the solid state than is the EP method.

The perturbation Hamiltonian H_N due to the nuclear magnetic moment is given by

$$H_N = \sum_i \frac{16\pi}{3} r_e r_N \hbar^2 \mathbf{I} \cdot \mathbf{S}_i \delta(\mathbf{r}_i), \quad (8)$$

where r_e and r_N are the magnetogyric ratios of the electron and nucleus, respectively. \mathbf{I} is the spin of the nucleus, \mathbf{S}_i and \mathbf{r}_i are the spin and position vectors of the i th electron. The summation extends over all electrons in the core states. The perturbation H_E can be written as

$$H_E = \sum_i H(i) = \sum_i \sum_k \alpha_{ik}, \quad (9)$$

where α_{ik} is defined by

$$\alpha_{ik} \phi_j(\mathbf{r}_i) = \psi_k(\mathbf{r}_i) \int \psi_k(\mathbf{r}_k) \frac{e^2}{|\mathbf{r}_i - \mathbf{r}_k|} \phi_j(\mathbf{r}_k) d\tau_k. \quad (10)$$

The summation over k extends over all valence electrons whose spin is parallel to core state ϕ_j and α_{ik} vanishes when operating on a core state j whose spin is not parallel to valence state k .

For the ground-state wave function we take a determinant built out of all the core states with spins both up and down. Since we are interested in effects linear in H_E we assume, as in previous work,¹⁷ that the down-spin core states are not perturbed while the up-spin core states are perturbed by H_E . The perturbed wave functions $\Psi_0 + \delta\Psi_E$ and $\Psi_0 + \delta\Psi_N$ are obtained from the zero-order wave function Ψ_0 by replacing the unperturbed one-electron wave functions in the determinant by perturbed one-electron wave functions and keeping terms up to first order.

Remembering that we have only one core (1s) for the Be atom and following the adaptation¹⁷ of Dalgarno's procedure for perturbed many-electron systems to the present problem, we obtain

$$\delta\psi_{1s,N} = A \delta\phi_{1s,N}, \quad (11)$$

where

$$A = (16\pi/3) r_e r_N \hbar^2 I_z m_s \quad (12)$$

with $m_s = \frac{1}{2}$ for up-spin core states and $m_s = -\frac{1}{2}$ for the down-spin state, and $\delta\phi_{1s,N}$ is given by the solution to the following equation

$$\left(-\nabla^2 + \frac{\nabla^2 \psi_{1s}}{\psi_{1s}} \right) \delta\phi_{1s,N} = -[\delta(\mathbf{r}) - \langle \psi_{1s} | \delta(\mathbf{r}) | \psi_{1s} \rangle] \psi_{1s}. \quad (13)$$

This is a second-order linear inhomogeneous equation for $\delta\phi_{1s,N}$, and can be solved by standard numerical techniques. However, in the present case since ψ_{1s} does not have any nodes and $\delta\phi_{1s,N}$ has the same angular dependence as ψ_{1s} one can use an especially simple procedure which requires only the evaluation of some integrals. This procedure is detailed in the Appendix.²² It only applies to problems in which the ground-state wave function is nodeless and the perturbation in the wave function has the same angular dependence as the zero-order wave function. Writing

$$\psi_{1s} = R_{1s} Y_0^0(\theta, \phi) = \frac{P_{1s}}{r} \frac{1}{\sqrt{4\pi}} \quad (14)$$

and

$$\delta\phi_{1s,N} = \delta R_{1s,N} Y_0^0(\theta, \phi) = \frac{\delta P_{1s,N}}{r} \frac{1}{\sqrt{4\pi}}. \quad (15)$$

The expression for $\delta\phi_{1s,N}$ obtained by this procedure is then the following:

$$\delta\phi_{1s,N} = \frac{1}{\sqrt{4\pi}} \frac{P_{1s}}{r} \left\{ \int_{\infty}^r F(r) dr + \int_{\infty}^0 P_{1s}^2(r) dr \int_{\infty}^r F(r) dr \right\}, \quad (16)$$

where $F(r)$ is given by

$$F(r) = -\frac{\langle \psi_{1s} | \delta(\mathbf{r}) | \psi_{1s} \rangle}{P_{1s}^2(r)} \int_{\infty}^r P_{1s}^2(r) dr. \quad (17)$$

$\delta\phi_{1s,N}$ was then solved numerically from Eq. (16) using Goodings¹⁹ calculated restricted Hartree-Fock wave function of the Be atom for ψ_{1s} . A plot of the wave functions $\delta P_{1s,N}$ and P_{1s} is given in Fig. 1. The general behavior of $\delta P_{1s,N}$ is very much the same as that obtained¹⁷ for Li as is to be expected.

Having obtained $\delta\phi_{1s,N}$ one can calculate $E_{eN}^{(2)}$ from Eq. (3) with H_E defined as in Eq. (9). In the Be atom $1s^2 2s 2p(^3P_2)$ state with two unpaired valence electrons,

²² This procedure is similar to a general method developed by P. J. Price [Proc. Phys. Soc. (London) **A67**, 383 (1954)]. We have presented this procedure in the Appendix to make it understandable in the present context.

TABLE I. List of contributions to hyperfine constants in Mc/sec for the 2P_2 term of the Be $1s^22s2p$ state.

	Core-polarization contribution			Direct 2s contribution	Total contact contribution	Dipolar contribution	Total
	a_c^{2s}	a_c^{2p}	$a_c = a_c^{2s} + a_c^{2p}$				
Goodings ^a			-14.7	-98.8	-113.5	-8.8	-122.3
This paper	-21.1	8.0	-13.1	-98.8	-111.9	-8.8	-120.7
Experimental ^b							-124.54

^a Reference 19.^b Reference 20.

H contains two parts, one from the $2s$ electron and the other from the $2p$ electron. Specifically, we have

$$H_E = H_{2s} + H_{2p}, \quad (18)$$

where

$$H_{2s} = -\frac{\psi_{2s}(\mathbf{r}_1)}{\psi_{1s}(\mathbf{r}_1)} \int \psi_{2s}^*(\mathbf{r}_2) \frac{e^2}{r_{12}} \psi_{1s}(\mathbf{r}_2) d\tau_2 \quad (19)$$

and

$$H_{2p} = -\frac{\psi_{2p}(\mathbf{r}_1)}{\psi_{1s}(\mathbf{r}_1)} \int \psi_{2p}^*(\mathbf{r}_2) \frac{e^2}{r_{12}} \psi_{1s}(\mathbf{r}_2) d\tau_2. \quad (20)$$

In Eqs. (18), (19), and (20), the operators H_E , H_{2s} , and H_{2p} are one-electron operators. Using Eqs. (11) and (18), one gets

$$E_{eN}^{(2)} = 2A \langle \delta\phi_{1s,N} | H_{2s} | \psi_{1s} \rangle + 2A \langle \delta\phi_{1s,N} | H_{2p} | \psi_{1s} \rangle. \quad (21)$$

To evaluate Eq. (21), we apply the usual technique of expanding $1/r_{12}$ in various spherical harmonics and performing the proper angular integrations. The final radial integrals to be evaluated are then

$$\begin{aligned} \langle \delta\phi_{1s,N} | H_{2s} | \psi_{1s} \rangle &= -2 \int_0^\infty P_{2s}(r_1) \delta P_{1s,N}(r_1) dr_1 \\ &\times \left\{ \frac{1}{r_1} \int_0^{r_1} P_{2s}(r_2) P_{1s}(r_2) dr_2 \right. \\ &\quad \left. + \int_{r_1}^\infty \frac{P_{2s}(r_2) P_{1s}(r_2)}{r_2} dr_2 \right\} \quad (22) \end{aligned}$$

and

$$\begin{aligned} \langle \delta\phi_{1s,N} | H_{2p} | \psi_{1s} \rangle &= -\frac{2}{3} \int_0^\infty P_{2p}(r_1) \delta P_{1s,N}(r_1) dr_1 \\ &\times \left\{ \frac{1}{r_1^2} \int_0^{r_1} r_2 P_{2p}(r_2) P_{1s}(r_2) dr_2 \right. \\ &\quad \left. + r_1 \int_{r_1}^\infty \frac{P_{2p}(r_2) P_{1s}(r_2)}{r_2^2} dr_2 \right\}. \quad (23) \end{aligned}$$

After performing these integrals, we obtained the numerical results

$$2 \langle \delta\phi_{1s,N} | H_{2s} | \psi_{1s} \rangle = 2 \times (0.067314) = 0.134628, \quad (24)$$

$$2 \langle \delta\phi_{1s,N} | H_{2p} | \psi_{1s} \rangle = 2 \times (-0.02545) = -0.0509, \quad (25)$$

where the zero-order radial wave functions p_{1s} , p_{2s} , and p_{2p} were taken from Goodings' restricted Hartree-Fock calculations.¹⁹

The total contribution to $E_{eN}^{(2)}$ is therefore $E_{eN}^{(2)}$ $A(0.08373)$. This compares very favorably with Goodings' value¹⁹ of $A(0.094)$ obtained by the UHF procedure.

The contribution a_c , in cycles, to the magnetic hyperfine coupling constant from the core polarization can be obtained from the formula

$$a_c = E_{eN}^{(2)} / IJh, \quad (26)$$

where J is the total angular momentum quantum number. From our results we found for beryllium, $a_c = -13.1$ Mc/sec.

In Table I we have listed for comparison the core-polarization contribution to the hyperfine constant obtained by us as well as Goodings' UHF results. For the sake of completeness we have also listed the direct, contact and dipolar contribution from the $2s$ and $2p$ states.

From Table I and Eqs. (24) and (25) it can be noticed that the core-polarization contribution from the $1s$ state is the difference of two numbers, one arising from the influence of the $2s$ polarizing electron and the other due to the $2p$ polarizing electron. It is therefore gratifying that the net a_c is within about 12% of the UHF result. This observation bears out our expectation that the perturbation approach would be better for Be than for Li. It would be interesting to compare the individual contributions from the $2s$ and $2p$ polarizing electrons for the MP and UHF methods. Unfortunately, Goodings has not presented these numbers for the UHF method.

From a study of the results in the two states of the Li atom ($1s^22s$ and $1s^22p$) and in the Be atom ($1s^22s2p$), it appears that the $2s$ valence electron produces a positive core polarization when interacting with the $1s$ state while a $2p$ electron produces a negative core polarization in the $1s$ state. A similar observation also applies to the Li metal where it was found that the s and p parts of the conduction electron produce positive and negative core polarization, respectively. The d part of the wave function produces a relatively small and negative core polarization. The opposite behavior of the s and p electron can be understood from the sign of the product of the valence and core wave function in the important region where they overlap significantly. It is this region that makes the most important contribution to the exchange potential H_E which ultimately determines the

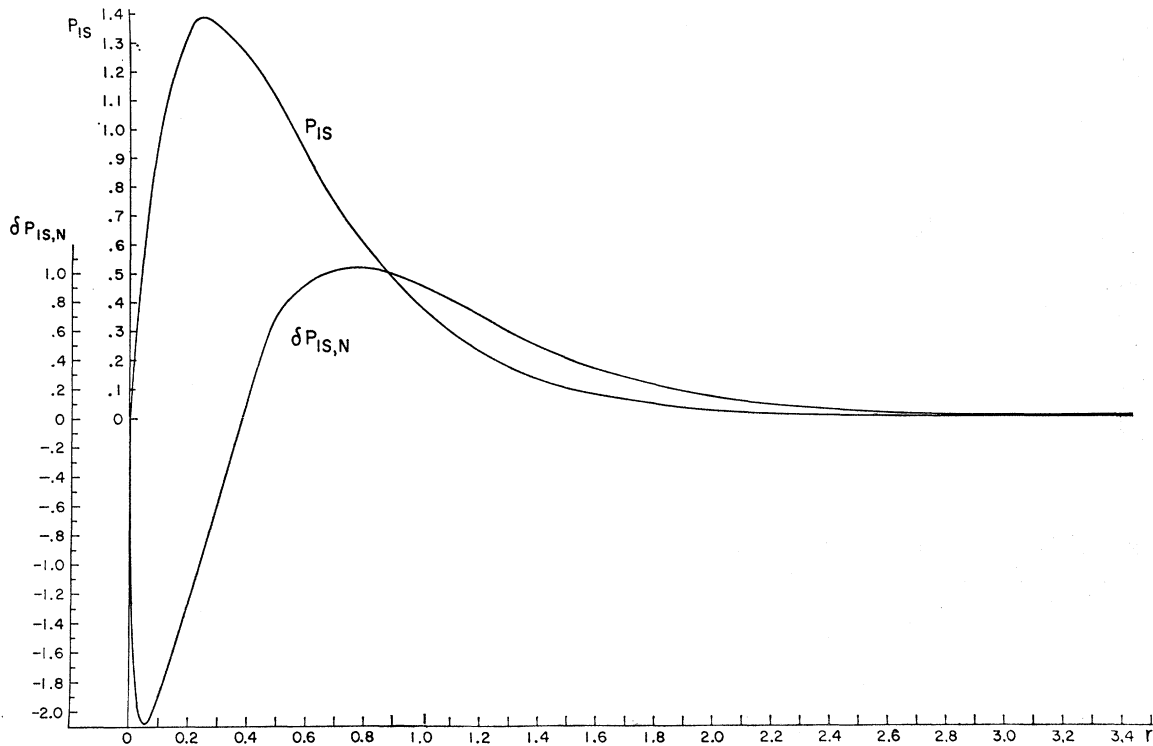


Fig. 1. Plot of unperturbed wave function P_{1s} , and first-order perturbed wave function $\delta P_{1s,N}$ as function of r for the Be atom $1s^2 2s 2p$ configuration.

core polarization contribution. Since the $2s$ wave function has a node while the $2p$ does not, the difference in the signs of their core polarization contribution is understandable. These observations seem to be borne out also by our calculation on Be metal in Sec. IV and permit us to arrive at some significant conclusions about the Knight shift in Be metal.

III. CONDUCTION-ELECTRON WAVE FUNCTIONS FOR BERYLLIUM METAL

In order to calculate the Knight shift in Be metal, a knowledge of the wave functions of the conduction electrons and the Fermi surface is needed. As mentioned in the Introduction, earlier band-structure calculations of Be metal by the orthogonalized-plane-wave method, particularly the most recent one by Loucks and Cutler,⁸ have led to fairly good agreement between observed macroscopic properties and theoretical predictions. We therefore chose the OPW procedure, to determine the conduction-electron wave functions.

One of the important objections that has been leveled at the OPW method in the past has been its slow convergence. However, as Heine²³ has emphasized, the slow convergence was found in many cases to be due to a poor choice of core wave functions which were used in

the construction of the OPW function. Heine has shown that a considerable improvement in the convergence of the OPW method can be attained if one chooses the crystal-core wave functions which are lower energy eigenfunctions in the conduction-electron potential. This choice of crystal-core states was used by Loucks and Cutler⁸ as well as by earlier workers⁷ in the OPW calculation on Be. Loucks and Cutler, however, went one step further and made the conduction potential self-consistent with respect to the crystal-core function using single OPW wave functions in the computation of the potential. The problem of making the calculation self-consistent with respect to the conduction-electron wave functions at different points of the band is computationally formidable and has not yet been done. Since we were not interested in improving upon the energy-calculation of Loucks and Cutler but in determining wave functions for the conduction electrons and studying the convergence properties of the energies and wave functions, we have made use of the conduction-electron potential that Loucks and Cutler obtained in their last iteration, starting with the potential determined by Pomerantz and Das.²

The one-electron potential seen by the conduction electron can be written as

$$V_c(\mathbf{r}) = \sum_{\nu} V(|\mathbf{r} - \mathbf{R}_{\nu}|), \quad (27)$$

²³ V. Heine, Proc. Roy. Soc. (London) A240, 354 (1957).

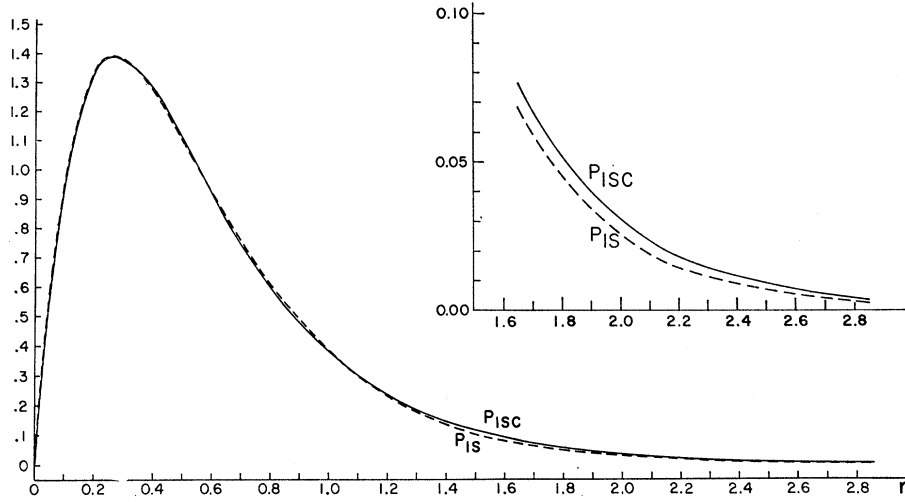


FIG. 2. Plot of the radial parts of the crystal-core wave function P_{1sc} and the atomic wave function P_{1s} as a function of r for Be metal.

where $V(r)$ is taken from Loucks and Cutler.⁸ To construct the OPW we require crystal-core wave functions $\psi_c(\mathbf{r})$ which are the lower energy eigenfunctions of the conduction-electron Hamiltonian. Thus,

$$H\psi_c = E_c\psi_c, \quad (28)$$

where H is the Hamiltonian for conduction electrons.

$$H = -\nabla^2 + V_c(\mathbf{r}). \quad (29)$$

For the crystal-core wave functions, it is convenient to use the Bloch functions

$$\psi_c = \frac{1}{\sqrt{(2N)}} \sum_{\nu} \exp(i\mathbf{k} \cdot \mathbf{R}_{\nu}) U_{1s}(\mathbf{r} - \mathbf{R}_{\nu}), \quad (30)$$

where \mathbf{R}_{ν} is the position vector of the nucleus at the ν th lattice point and ν goes over all the lattice points in the crystal. If the potentials $V(|\mathbf{r} - \mathbf{R}_{\nu}|)$ on adjacent sites do not have significant overlap and also if the functions $U_{1s}(\mathbf{r} - \mathbf{R}_{\nu})$ on neighboring ions do not overlap appreciably, one can then write

$$[-\nabla^2 + V(r)]U_{1s}(r) = E_c U_{1s}(r). \quad (31)$$

On writing

$$U_{1s} = (P_{1sc}/r) Y_0^0(\theta, \phi), \quad (32)$$

Equation (31) reduces to

$$[-d^2/dr^2 + V(r)]P_{1sc}(r) = E_c P_{1sc}(r). \quad (33)$$

Equation (33) was then solved numerically for both E_c and $P_{1sc}(r)$ by standard technique. We have made use of the program originally written by Cooley²⁴ and modified by Zare and Cashion²⁵ for this purpose. The results so obtained were in close agreement with those of Loucks and Cutler.

We like to remind the reader that the crystal-core wave function U_{1s} as obtained from Eq. (32) is quite distinct from the actual-core wave function which is an eigenfunction of the potential seen by the core electrons. This distinction is important in Sec. IV dealing with the core-polarization calculation where we have used both crystal-core and the actual-core wave functions. The actual-core wave function is very close to the $1s$ wave function ψ_{1s} for the Be atom. A comparison of the radial parts of the crystal-core wave function $P_{1sc}(r)$ and the atomic wave function $P_{1s}(r)$ is presented in Fig. 2.

Once the crystal-core wave function is determined, one can obtain orthogonalized plane waves of the form²⁶

$$\chi_{\mathbf{k}} = \frac{\exp(i\mathbf{k} \cdot \mathbf{r})}{\sqrt{(N\Omega)}} - \frac{1}{\sqrt{N}} A_{1s}(\mathbf{k}) \times \sum_{\nu} \exp(i\mathbf{k} \cdot \mathbf{R}_{\nu}) U_{1s}(\mathbf{r} - \mathbf{R}_{\nu}), \quad (34)$$

with

$$A_{1s}(\mathbf{k}) = \left(\frac{4\pi}{\Omega}\right)^{(1/2)} \int_0^{\infty} r P_{1sc}(r) j_0(kr) dr, \quad (35)$$

where Ω is the volume of the unit cell and N is the number of unit cells in the crystal. The symbol $j_0(kr)$ refers to spherical Bessel function of order zero.

To obtain the conduction electron wave function one has to take a linear combination of OPW's.

$$\psi_{\text{trial}}(\mathbf{k}) = \sum_i B_i \chi_{\mathbf{k}_i}, \quad (36)$$

where $\mathbf{k}_i = \mathbf{k} + \mathbf{K}_i$, \mathbf{K}_i begin a reciprocal lattice vector. The coefficients B_i can be determined after solving the requisite secular equation. A sufficient number of reciprocal lattice vectors should be included to obtain convergence. Twenty-three reciprocal lattice vectors

²⁴ J. W. Cooley, *Math. Computation* **15**, 363 (1961).

²⁵ R. N. Zare and J. K. Cashion, University of California Radiation Laboratory Technical Report No. 10881 (unpublished).

²⁶ T. O. Woodruff, *Solid State Physics*, edited by F. Seitz and D. Turnbull (Academic Press Inc., New York, 1957), Vol. 4.

TABLE II. Convergence tests of energy eigenvalues and variational parameters of the wave function at the symmetry points of Γ and H of the Brillouin zone in Be metal.

Representation	No. of OPW's involved	Order of secular Eq. (No. of SLCOPW's)	Energy ^a	Variational parameters a_i defined in Eq. (37)					
				a_1		a_2		a_3	
				Real	Imaginary	Real	Imaginary	Real	Imaginary
Γ_4^-	3	1	0.9538	1.0723	0.0000
	9	2	0.9477	1.0659	0.0000	-0.0500	-0.0289
	23	3	0.9464	1.0642	0.0000	-0.0498	-0.0288	0.0115	-0.0198
	6	1	0.9387	{1.0000 1.0000}	{0.0000 0.0000}
H_1	12	2	0.9313	{0.9979 0.9979}	{0.0000 0.0000}	{0.0652 -0.0652}	{0.0000 0.0000}
	18	3	0.9158	{0.9948 0.9948}	{0.0000 0.0000}	{0.0676 -0.0676}	{0.0000 0.0000}	{0.0384 0.0384}	{-0.0666 -0.0666}

^a Refers to the bottom of the band which is at -0.1893 Ry. The Fermi energy obtained by Loucks and Cutler (Ref. 8) is $E_F = 0.901$ Ry.

were included in the summation by Loucks and Cutler⁸ in their energy band calculation in Be. They made no use of group theory to factor the secular equation perhaps because group theory is of no help at general points in \mathbf{k} space. Also they did not determine the B_i 's since they are only interested in the energy bands. In our calculation, however, we are more interested in assessing the importance of core-polarization effects than in their exact quantitative evaluation; we have therefore performed our calculation at a few points of symmetry. At these points group-theoretical factorization has considerable merit not only because it reduces drastically the amount of work involved in computing matrix elements and solving a much lower order secular equation but also from the point of view of accuracy. For example, regarding the Γ_4^- level of the Γ point, with the help of group theory, one only has 3 coefficients to solve instead of 23 B_i 's. The other twenty coefficients are determined in terms of the calculated three using exact ratios between the coefficients which are determined from the group of \mathbf{k} . Since there is inevitably some error involved in the numerical methods for solving the secular equation, a third-order secular equation would naturally involve less inaccuracy than one of 23rd order.

Thus we set up the trial wave function built out of symmetrized linear combination of orthogonalized plane waves (SLCOPW) which are adequate for the irreducible representation at the symmetry points in which we are interested

$$\psi_{\text{trial}} = \sum_l a_l S_l^{|\mathbf{k}_l|}, \quad (37)$$

where the a_l 's denote the variational parameters of the trial wave function and $S_l^{|\mathbf{k}_l|}$ is the proper (SLCOPW) for a fixed $|\mathbf{k}_l|$ value.

$$S_l^{|\mathbf{k}_l|} = \sum_{\mathbf{k}_q} C_{\mathbf{k}_q}{}^l \chi_{\mathbf{k}_q}{}^l \quad (\text{for all } \mathbf{k}_q \text{ that } |\mathbf{k}_q| = |\mathbf{k}_l|), \quad (38)$$

where the $C_{\mathbf{k}_q}{}^l$'s are the symmetrized coefficients determined by the group theory and $\chi_{\mathbf{k}_q}{}^l$ is the usual one-OPW expression as given in Eq. (34).

The secular equation requires the calculation of the matrix elements (S_l', HS_l) and (S_l', S_l) . Following the usual procedure, we obtain the following results:

$$(S_l', HS_l) = \sum_{\mathbf{k}_q' \mathbf{k}_q} C_{\mathbf{k}_q'}{}^{l'} * C_{\mathbf{k}_q}{}^l \times \left[|\mathbf{k}_q|^2 \delta_{\mathbf{q}\mathbf{q}'} + \{VF_{\mathbf{q}\mathbf{q}'} - E_c B_l' B_l\} \times \frac{4\pi}{\Omega} \{1 + \exp i(\mathbf{k}_q - \mathbf{k}_q') \cdot \boldsymbol{\tau}\} \right] \quad (39)$$

and

$$(S_l', S_l) = \sum_{\mathbf{k}_q' \mathbf{k}_q} C_{\mathbf{k}_q'}{}^{l'} * C_{\mathbf{k}_q}{}^l \left[|\mathbf{k}_q|^2 \delta_{\mathbf{q}\mathbf{q}'} - B_l' B_l \frac{4\pi}{\Omega} \{1 + \exp i(\mathbf{k}_q - \mathbf{k}_q') \cdot \boldsymbol{\tau}\} \right], \quad (40)$$

where

$$VF_{\mathbf{q}\mathbf{q}'} = \frac{1}{|\mathbf{k}_q - \mathbf{k}_q'|} \int_0^\infty V(r) \sin(|\mathbf{k}_q - \mathbf{k}_q'| r) r dr, \quad (41)$$

$$B_l = \frac{1}{|\mathbf{k}_l|} \int_0^\infty P_{1sc}(r) \sin(|\mathbf{k}_l| r) dr, \quad (42)$$

$$B_l' = \frac{1}{|\mathbf{k}_l'|} \int_0^\infty P_{1sc}(r) \sin(|\mathbf{k}_l'| r) dr, \quad (43)$$

and $\boldsymbol{\tau}$ is the distance (nonprimitive translation) between the two atoms contained in a unit cell. We have made use of the symmetrized coefficients $C_{\mathbf{k}_q}{}^l$ tabulated at six symmetry points of the Brillouin zone by Falicov²⁷ for his band-structure calculation on magnesium.

The secular equation

$$\det |(S_l', HS_l) - E(S_l', S_l)| = 0 \quad (44)$$

²⁷ L. M. Falicov, Phil. Trans. Roy. Soc. A255, 55 (1962).

was then set up and evaluated for the Γ_4^- representation at the Γ point and the two degenerate representations of H_1 at the H point. The resulting polynomials were then solved for the lowest energy eigenvalues because these were close to the Fermi energy. The selection of Γ_4^- and H_1 representations also provide a good sampling of the Fermi surface since the former is s -like and the latter non- s -like. The corresponding eigenvectors (the variational parameters a_i) were then obtained by solving a set of simultaneous equations. All these numerical calculations were complicated by the fact that τ is a nonprimitive translation vector and consequently one has to deal with complex algebra and complex numbers. The results obtained together with the convergence tests are given in Table II.

From Table II we notice that both the energy value and the variational parameters in the wave function showed extremely good convergence with increasing order of secular equation and consequently increasing number of OPW's involved. The convergence of the variational parameters have particular importance in the evaluation of the Knight shift which will be discussed in the next section.

IV. KNIGHT SHIFT AND CORE POLARIZATION IN BERYLLIUM METAL

The usual expression for the Knight shift due to the conduction electrons is by

$$(\Delta H/H)_{\text{direct}} = (8\pi/3)\chi_p V \langle |\psi_F(0)|^2 \rangle_{\text{av}}, \quad (45)$$

where χ_p is the spin paramagnetic susceptibility, $\langle |\psi_F(0)|^2 \rangle_{\text{av}}$ is the average electron density at the nucleus from the electrons at the Fermi surface and V is the volume of the crystal in which ψ is normalized. A convenient expression for $\langle |\psi_F(0)|^2 \rangle_{\text{av}}$ for purposes of computation has been given by Callaway²⁸

$$\langle |\psi_F(0)|^2 \rangle_{\text{av}} = [4\pi^3 n(\mu)]^{-1} \times \int |\psi(\mathbf{k}, 0)|^2 (|\nabla_{\mathbf{k}} E|)^{-1} dS_F, \quad (46)$$

where $n(\mu)$ is the density of states on the Fermi surface and the integral extends over the whole Fermi surface.

From Eq. (46) it is clear that an accurate evaluation of $\langle |\psi_F(0)|^2 \rangle_{\text{av}}$ requires (i) a knowledge of the Fermi surface, (ii) the variation of E with respect to \mathbf{k} , and (iii) the variation of the conduction-electron wave function $\psi_{\mathbf{k}}$ with respect to \mathbf{k} as one traverses the Fermi surface. Our aim in this paper is not an accurate evaluation of the Knight shift but rather an investigation of sources of error in the direct Knight shift and the understanding of the role of core polarization to determine if the core-polarization contribution can possibly counteract the direct contribution to the Knight shift so as to

give the vanishingly small total Knight shift observed experimentally. We have therefore considered the lowest level of the Γ_4^- representation and the two degenerate representations of H_1 . The Γ_4^- representation has primarily s character and therefore contributes a substantial direct Knight shift. The H_1 representations on the other hand, have no s character, and therefore produce zero direct Knight shift. Any other points, on or close to Fermi surface, will lie between these two cases. We therefore feel that for an understanding of the direct and core-polarization contributions to the Knight shift the study of the Γ_4^- and H_1 representations is most informative.

In the calculation of the direct Knight shift using Eq. (45) we need a knowledge of the spin susceptibility χ_p . Feher and Kip²⁹ obtained a value of $\chi_p = 2 \times 10^{-7}$ cgs volume units from the area under the electron-spin-resonance signal in Be metal. This value is about a factor of 3 smaller than the calculated value using the result of the density of states at the Fermi surface obtained by both Loucks and Cutler⁸ and Herring and Hill⁷ by means of the following expression⁵

$$\chi_p = \mu_B^2 n(\mu), \\ \chi_p = 6.86 \times 10^{-7}, \quad \text{cgs volume units.}$$

This value is in exact agreement with the result one gets from the experimental value of the low-temperature specific heat γ in Be metal³⁰ using the relation between χ_p and γ in the one-electron approximation

$$\gamma = \pi^2 k^2 n(\mu) / 3.$$

The disagreement between the spin-resonance value of χ_p and the theoretical value from the density-of-states calculation is somewhat disturbing. It could arise either out of some uncertainty in the evaluation of χ_p from the spin-resonance measurement or from the neglect of correlation effects in the calculation of χ_p . In the absence of definite information on this point we have tabulated our results on the Knight shift using the spin-resonance value.

$\chi_p = 2 \times 10^{-7}$ cgs volume units. To obtain the results for the Knight shift pertinent to the choice of $\chi_p = 6.86 \times 10^{-7}$ cgs volume units, we only have to multiply the tabulated results by a factor of 3.43.

The question of convergence in the predicted direct contribution to the Knight shift will be considered first. In Table III we have listed the calculated values of $\psi_F^2(0)$ and the direct Knight shift for different numbers of SLCOPW used for the Γ_4^- representation. It can be seen that the direct Knight shift for 3 SLCOPW's is only about 6% less than that for 1 SLCOPW. While we have not demonstrated the convergence for a general point, it is not unreasonable to expect that the calculated direct Knight shift would be quite rapidly con-

²⁸ J. Callaway, *Energy Band Theory* (Academic Press Inc., New York, 1964).

²⁹ G. Feher and A. F. Kip, *Phys. Rev.* **98**, 337 (1955).

³⁰ R. W. Hill and P. L. Smith, *Phil. Mag.* **44**, 636 (1953).

TABLE III. Convergence test of $(\Delta H/H)_{\text{direct}}$ for Γ_4^- level at symmetry point Γ in Be metal.

Order of secular Eq.	No. of OPW's involved	$\psi_{p^2}(0)$	$\left(\frac{\Delta H}{H}\right)_{\text{direct}}$
1	3	102.3758	0.01715%
2	9	95.6305	0.01602%
3	23	95.1694	0.01595%
		91.6885 ^a	0.01536% ^a

^a After being corrected for the normalization to the real-core states.

vergent with respect to the number of OPW's. This result is in contradiction with the conclusion arrived at by Schneider *et al.*⁴ in recent work. These authors concluded from their results for 1 and 3 SLCOPW's that the calculated Knight shift was very poorly convergent (see Fig. 2 of Ref. 4). Our result for 3 SLCOPW's agrees quite well with their result but our 1 SLCOPW result disagrees with theirs. The origin of this disagreement is probably due to a numerical error in their calculation. The good convergence we have obtained for the direct Knight shift leads us to believe that the OPW method does in fact give us a good representation of the conduction-electron wave function near the nucleus in a good metal. This conclusion will perhaps be inapplicable to semimetals and semiconductors and a combination of

tight-binding and OPW method proposed by Schneider *et al.*⁴ may therefore be desirable in those cases. For beryllium metal, we feel that the necessity for such a modification of the OPW method has not been demonstrated.

The last row in Table III gives the direct Knight shift after correcting for the lack of orthogonality between the conduction-electron wave function ψ_{cond} and the real-core wave function. This point has not been considered in earlier investigations so we shall explain it here briefly. The real-core wave function $\psi_{c,1s}$ is not expected to be significantly different from the atomic ψ_{1s} wave function. The overlap integral between the 23 OPW's and the real-core function was found to be

$$\langle \psi_{c,1s} | \psi_{\text{cond}} \rangle = -0.0027833.$$

Whenever one has two nonorthogonal states and needs the expectation value of one-electron operator it can be shown that one gets the same expectation value if one uses orthogonalized orbitals which have been orthogonalized by Schmidt's procedure.³¹ In the present case we found it convenient to orthogonalize the conduction wave function ψ_{cond} to the real-core wave function $\psi_{c,1s}$

$$\psi_{\text{ortho}} = \sum_l a_l S_{l, \text{ortho}} |k_l|, \quad (47)$$

with

$$S_{l, \text{ortho}} |k_l| = \sum_{k_q} C_{k_q}^l \chi_{k_q, \text{ortho}}^l \quad (\text{for all } \mathbf{k}_q \text{ that } |\mathbf{k}_q| = |\mathbf{k}_l|), \quad (48)$$

where

$$\chi_{k_q, \text{ortho}}^l = \frac{\exp(i\mathbf{k} \cdot \mathbf{r})}{\sqrt{(N\Omega)}} \frac{1}{\sqrt{N}} A_{1s}(k) \sum_{\nu} \exp(i\mathbf{k} \cdot \mathbf{R}_{\nu}) u_{1s}(\mathbf{r} - \mathbf{R}_{\nu}) - \frac{1}{\sqrt{N}} A_{1s}'(k) \sum_{\nu} \exp(i\mathbf{k} \cdot \mathbf{R}_{\nu}) \psi_{1s}(\mathbf{r} - \mathbf{R}_{\nu}), \quad (49)$$

with

$$A_{1s}'(k) = \left(\frac{4\pi}{\Omega}\right)^{1/2} \int_0^{\infty} r P_{1s}(r) j_0(kr) dr - A_{1s}(k) \int_0^{\infty} P_{1s}(r) P_{1s}(r) dr. \quad (50)$$

Using ψ_{ortho} we obtained the Knight shift as listed in the last row of Table III. The lack of orthogonality between conduction-electron wave function and the real-core function is thus seen to be minimal in its effect on the direct Knight shift.

It should be noted that this type of nonorthogonality contribution to the hyperfine interaction does not occur in atoms because the core and valence functions are orthogonal either owing to their angular parts (*s* and *p* states, for example) or when the angular part is the same, owing to the orthogonality condition imposed on the radial parts of the wave functions when solving the Hartree-Fock equation.

It is now clear that the vanishingly small Knight shift observed experimentally cannot be explained by errors in the direct Knight shift calculation. We therefore proceed to an investigation of the core-polarization contribution to the Knight shift. The procedure that will be followed is the MP method which has already been used for the Be atom in Sec. II and for the Li atom and Li metal in an earlier paper.¹⁷ In a similar manner as was done in Ref. 17,³² the core-polarization contribution to the Knight shift is given by

$$\left(\frac{\Delta H}{H}\right)_{cp} = \frac{8\pi}{3} \chi_p V (2 \text{Re} \langle \delta\phi_{c,1s} | H_E | \psi_{c,1s} \rangle), \quad (51)$$

³¹ B. S. Gourary and F. J. Adrian, Phys. Rev. **105**, 1180 (1957).

³² A negative sign was left out on the right-hand side of both Eqs. (43) and (47). The results in Table II are of correct sign.

with

$$H_E = -\frac{\psi_{\text{cond}}(r_1)}{\psi_{c,1s}(r_1)} \int \psi_{\text{cond}}^*(r_2) \frac{e^2}{r_{12}} \psi_{c,1s}(r_2) d\tau_2, \quad (52)$$

where $\text{Re}\langle \delta\phi_{c,1s} | H_E | \psi_{c,1s} \rangle$ means the real part of $\langle \delta\phi_{c,1s} | H_E | \psi_{c,1s} \rangle$.

In the calculation on Li metal the normalization was performed over the Wigner-Seitz sphere and the integral in Eq. (43) of Ref. 17 was also confined to the Wigner-Seitz sphere. In our present formulation, however, the integrals in Eqs. (51) and (52) extend over the whole crystal.

Introducing Bloch functions for the real-core and the perturbed wave function in the tight-binding approximation, we have

$$\psi_{c,1s}(r) = \frac{1}{\sqrt{(2N)}} \sum_{\nu'} \exp(i\mathbf{k} \cdot \mathbf{R}_{\nu'}) \psi_{1s}(\mathbf{r} - \mathbf{R}_{\nu'}) \quad (53)$$

and

$$\delta\phi_{c,1s}(r) = \frac{1}{\sqrt{(2N)}} \sum_{\nu} \exp(i\mathbf{k} \cdot \mathbf{R}_{\nu}) \delta\phi_{1s,N}(\mathbf{r} - \mathbf{R}_{\nu}), \quad (54)$$

with ψ_{1s} and $\delta\phi_{1s,N}$ defined as in Sec. II.

Making use of Eq. (37) for conduction-electron wave function ψ_{cond} and Eqs. (53) and (54) we get

$$\begin{aligned} \langle \delta\phi_{c,1s} | H_E | \psi_{c,1s} \rangle = & -\frac{1}{N} \sum_{l,l'} a_l a_{l'}^* \sum_{k_q k_{q'}} C_{k_q}^l C_{k_{q'}}^{l'*} \int \int \sum_{\nu} \exp(-i\mathbf{k}_q \cdot \mathbf{R}_{\nu}) \delta\phi_{1s,N}^*(\mathbf{r}_1 - \mathbf{R}_{\nu}) \\ & \times \chi_{k_q}^l(r_1) \chi_{k_{q'}}^{l'*}(r_2) \frac{1}{r_{12}} \sum_{\nu'} \exp(i\mathbf{k}_{q'} \cdot \mathbf{R}_{\nu'}) \psi_{1s}(\mathbf{r}_2 - \mathbf{R}_{\nu'}) d\tau_1 d\tau_2. \quad (55) \end{aligned}$$

In Eq. (55) we have two types of integrals: one in which all the localized orbitals are centered about the nucleus in question and another in which orbitals about adjacent centers are also involved. An examination of the order of magnitude of the contribution from the latter type of integrals indicates that they make a negligible contribution; we can therefore simplify Eq. (55) to the following form

$$\langle \delta\phi_{c,1s} | H_E | \psi_{c,1s} \rangle = -\frac{2}{N\Omega} \sum_{l,l'} a_l a_{l'}^* \sum_{k_q k_{q'}} C_{k_q}^l C_{k_{q'}}^{l'*} \int \int \delta\phi_{1s,N}(r_1) F(r_1) \frac{1}{r_{12}} F(r_2) \psi_{1s}(r_2) d\tau_1 d\tau_2, \quad (56)$$

with

$$F(r_1) = \exp(i\mathbf{k}_q \cdot \mathbf{r}_1) - (4\pi)^{1/2} B_l u_{1s}(r_1) \quad (57)$$

and

$$F(r_2) = \exp(-i\mathbf{k}_{q'} \cdot \mathbf{r}_2) - (4\pi)^{1/2} B_{l'} u_{1s}(r_2), \quad (58)$$

where B_l and $B_{l'}$ are given in Eqs. (42) and (43).

One can now make use of the expansion:

$$\frac{1}{r_{12}} = 4\pi \sum_{l=0}^{\infty} \frac{1}{2l+1} \frac{r_{<}^l}{r_{>}^{l+1}} \sum_{m=-l}^l Y_l^{m*}(\theta_1, \phi_1) Y_l^m(\theta_2, \phi_2), \quad (59)$$

and

$$e^{i\mathbf{k} \cdot \mathbf{r}} = 4\pi \sum_{l,m} i^l j_l(kr) Y_l^m(\theta_r, \phi_r) Y_l^{m*}(\theta_k, \phi_k), \quad (60)$$

and group the terms in Eq. (56) according to the values of l . These terms arise from the corresponding l parts of the ψ_{cond} and may be referred to as contributions from the s, p, d, \dots parts of the conduction-electron wave function. Thus, the $s(l=0)$ contribution to $\langle \delta\phi_{c,1s} | H_E | \psi_{c,1s} \rangle$ is

$$\langle \delta\phi_{c,1s} | H_E | \psi_{c,1s} \rangle_s = -\frac{2}{N\Omega} \sum_{l,l'} a_l a_{l'}^* \sum_{k_q k_{q'}} C_{k_q}^l C_{k_{q'}}^{l'*} \int \int \delta\phi_{1s,N}^*(r_1) F(r_1)_s \left(\frac{1}{r_{12}} \right)_s F(r_2)_s \psi_{1s}(r_2) d\tau_1 d\tau_2. \quad (61)$$

After carrying out all the angular integrations, Eq. (61) becomes

$$\begin{aligned} \langle \delta\phi_{c,1s} | H_E | \psi_{c,1s} \rangle_s = & -\frac{8\pi}{N\Omega} \sum_{l,l'} a_l a_{l'}^* \sum_{k_q k_{q'}} C_{k_q}^l C_{k_{q'}}^{l'} \int_0^\infty \delta P_{1s,N}(r_1) \left\{ \frac{\sin(|\mathbf{k}_q| r_1)}{|\mathbf{k}_q|} - B_l P_{1sc}(r_1) \right\} dr_1 \\ & \times \left[\frac{1}{r_1} \int_0^{r_1} P_{1s}(r_2) \left\{ \frac{\sin(|\mathbf{k}_{q'}| r_2)}{|\mathbf{k}_{q'}|} - B_{l'} P_{1sc}(r_2) \right\} dr_2 + \int_{r_1}^\infty \frac{P_{1s}(r_2)}{r_2} \left\{ \frac{\sin(|\mathbf{k}_{q'}| r_2)}{|\mathbf{k}_{q'}|} - B_{l'} P_{1sc}(r_2) \right\} dr_2 \right]. \quad (62) \end{aligned}$$

Similarly, the $p(l=1)$ contribution to $\langle \delta\phi_{c,1s} | H_E | \psi_{c,1s} \rangle$ is

$$\langle \delta\phi_{c,1s} | H_E | \psi_{c,1s} \rangle_p = -\frac{2}{N\Omega} \sum_{l,l'} a_l a_{l'}^* \sum_{k_q k_{q'}} C_{k_q}^l C_{k_{q'}}^{l'} \int \int \delta\phi_{1s,N}^*(r_1) F(r_1) P\left(\frac{1}{r_{12}}\right) F(r_2) P \psi_{1s}(r_2) d\tau_1 d\tau_2. \quad (63)$$

After making use of the following relation:

$$P_l(\cos\gamma_{qq'}) = \frac{4\pi}{2l+1} \sum_{m=-l}^l Y_l^{m*}(\theta_{k_q}, \phi_{k_q}) Y_l^m(\theta_{k_{q'}}, \phi_{k_{q'}}), \quad (64)$$

and carrying out the angular integrations, Eq. (64) becomes

$$\begin{aligned} \langle \delta\phi_{c,1s} | H_E | \psi_{c,1s} \rangle_P = & -\frac{8\pi}{N\Omega} \sum_{l,l'} a_l a_{l'}^* \sum_{k_q k_{q'}} C_{k_q}^l C_{k_{q'}}^{l'} (\cos\gamma_{qq'}) \\ & \times \int_0^\infty \frac{\delta P_{1s,N}^*(r_1)}{|\mathbf{k}_q|^2 r_1} \{ \sin(|\mathbf{k}_q| r_1) - |\mathbf{k}_q| r_1 \cos(|\mathbf{k}_q| r_1) \} dr_1 \left[\frac{1}{r_1^2} \int_0^{r_1} \frac{P_{1s}(r_2)}{|\mathbf{k}_{q'}|^2} \{ \sin(|\mathbf{k}_{q'}| r_2) - |\mathbf{k}_{q'}| r_2 \cos(|\mathbf{k}_{q'}| r_2) \} dr_2 \right. \\ & \left. + r_1 \int_{r_1}^\infty \frac{P_{1s}(r_2)}{|\mathbf{k}_{q'}|^2 r_2^3} \{ \sin(|\mathbf{k}_{q'}| r_2) - |\mathbf{k}_{q'}| r_2 \cos(|\mathbf{k}_{q'}| r_2) \} dr_2 \right]. \quad (65) \end{aligned}$$

Similarly, we obtain the $d(l=2)$ contribution to $\langle \delta\phi_{c,1s} | H_E | \psi_{c,1s} \rangle$ as

$$\langle \delta\phi_{c,1s} | H_E | \psi_{c,1s} \rangle_d = -\frac{2}{N\Omega} \sum_{l,l'} a_l a_{l'}^* \sum_{k_q k_{q'}} C_{k_q}^l C_{k_{q'}}^{l'} \int \int \delta\phi_{1s,N}^*(r_1) F(r_1) d\left(\frac{1}{r_{12}}\right) F(r_2) d \psi_{1s}(r_2) d\tau_1 d\tau_2, \quad (66)$$

$$\begin{aligned} \langle \delta\phi_{c,1s} | H_E | \psi_{c,1s} \rangle_d = & -\frac{4\pi}{N\Omega} \sum_{l,l'} a_l a_{l'}^* \sum_{k_q k_{q'}} C_{k_q}^l C_{k_{q'}}^{l'} (3 \cos^2 \gamma_{qq'} - 1) \\ & \times \int_0^\infty \frac{\delta P_{1s,N}^*(r_1)}{|\mathbf{k}_q|^3 r_1^2} \{ (3 - |\mathbf{k}_q|^2 r_1^2) \sin(|\mathbf{k}_q| r_1) - 3 |\mathbf{k}_q| r_1 \cos(|\mathbf{k}_q| r_1) \} dr_1 \\ & \times \left[\frac{1}{r_1^3} \int_0^{r_1} \frac{P_{1s}(r_2)}{|\mathbf{k}_{q'}|^3} \{ (3 - |\mathbf{k}_{q'}|^2 r_2^2) \sin(|\mathbf{k}_{q'}| r_2) - 3 |\mathbf{k}_{q'}| r_2 \cos(|\mathbf{k}_{q'}| r_2) \} dr_2 \right. \\ & \left. + r_1^2 \int_{r_1}^\infty \frac{P_{1s}(r_2)}{|\mathbf{k}_{q'}|^3 r_2^5} \{ (3 - |\mathbf{k}_{q'}|^2 r_2^2) \sin(|\mathbf{k}_{q'}| r_2) - 3 |\mathbf{k}_{q'}| r_2 \cos(|\mathbf{k}_{q'}| r_2) \} dr_2 \right]. \quad (67) \end{aligned}$$

Equations (62), (65), and (67) were then evaluated for the Γ_4^- representation and also the two degenerate representations of H_1 using $\delta P_{1s,N}^*(r_1)$ obtained in Sec. II. The core-polarization contribution to the Knight shift was then calculated using Eq. (51). The results together with the convergence test are listed in Table IV.

V. DISCUSSION

From Table IV it can be seen that for the Γ_4^- representation the core-polarization contribution to the Knight shift is only 18% of that due to the direct contribution. For one of the H_1 representations the core-polarization contribution is 49% of the direct Knight

TABLE IV. List of contributions to the Knight shift for the Γ_4^- representation and the two degenerate representations of H_1 for Be metal.

Representation	No. of OPW's involved	Order of secular Eq.	Direct contribution $(\Delta H/H)_{\text{direct}}$	Core polarization s part $(\Delta H/H)_{cs}$	Core polarization p part $(\Delta H/H)_{cp}$	Core polarization d part $(\Delta H/H)_{cd}$	Total $(\Delta H/H)_{\text{total}}$
Γ_4^-	3	1	0.01715%	0.00301%	0.00000%	-0.00002%	0.02014%
	9	2	0.01602%	0.00283%	0.00000%	-0.00002%	0.01883%
	23	3	0.01595%	0.00279%	0.00000%	-0.00002%	0.01871%
			0.01536% ^a	0.00260% ^a	0.00000% ^a	-0.00002% ^a	0.01794% ^a
H_1	6	1	0.00000%	0.00000%	-0.00058%	-0.00002%	-0.00060%
			0.00000%	0.00000%	0.00000%	-0.00002%	-0.00002%
	12	2	0.00000%	0.00000%	-0.00063%	-0.00002%	-0.00065%
			0.00000%	0.00000%	0.00000%	-0.00001%	-0.00001%
	18	3	0.00000%	0.00000%	-0.00058%	-0.00003%	-0.00061%
		0.00000%	0.00000%	0.00000%	-0.00001%	-0.00001%	

^a After being corrected for the orthogonality to the real core.

shift at Γ point with opposite sign. For the other H_1 representation the core-polarization effect is negligible. It thus appears as anticipated from the results for the Be atom and for the Li atom and Li metal that the core polarization is indeed positive for the conduction-electron wave function with s character and negative for the conduction-electron wave function with p character. At a general point on the Fermi surface, the conduction-electron wave function will have both s and p parts. (d and higher components are seen to be negligible in effect from the core polarization contribution of the d -like degenerate H_1 representation in Table IV.) Unless the p part is abnormally large, one would expect a positive Knight shift from the combined effects of direct and core-polarization contributions. From Loucks and Cutler's results⁸ it is clear that very little of the Fermi surface occurs around the H point while a relatively large part resides around the Γ point. We can therefore conclude from our investigations that the core-polarization effect cannot neutralize the direct contribution to the Knight shift to bring the net result in agreement with the vanishingly small experimental value. The reason for the small observed Knight shift has therefore to be sought elsewhere. The qualitative explanation offered by Das and Sondheimer¹³ from a consideration of the Landau-type contribution seems promising. To make a quantitative analysis one would have to adopt a formulation of the type developed by Hebborn and Stephen¹⁵ for the Bloch wave function. In their present form, however, the expressions developed by Hebborn and Stephen require much more detailed knowledge of energy bands and wave functions than is currently available. Finally we should remind the reader that our present calculations of the direct and core-polarization contribution to the Knight shift are strictly in the spirit of a one-electron picture. It is possible that the introduction of correlation effects can affect the results significantly. However, there is no procedure currently available for a proper inclusion of many-body

effects in the calculation of conduction-electron wave functions.

APPENDIX

From Eq. (13), we have

$$\left(-\nabla^2 + \frac{\nabla^2 \psi_{1s}}{\psi_{1s}}\right) \delta \phi_{1s,N} = -[\delta(\mathbf{r}) - \langle \psi_{1s} | \delta(\mathbf{r}) | \psi_{1s} \rangle] \psi_{1s}. \quad (\text{A1})$$

If we define the following relations

$$\psi_{1s} = R_{1s} Y_0^0(\theta, \phi) = \frac{P_{1s}}{r} \frac{1}{\sqrt{4\pi}}, \quad (\text{A2})$$

$$\delta \phi_{1s,N} = \delta R_{1s,N} Y_0^0(\theta, \phi) = \frac{\delta P_{1s,N}}{r} \frac{1}{\sqrt{4\pi}}, \quad (\text{A3})$$

and

$$\delta P_{1s,N} = (\delta \rho) P_{1s}. \quad (\text{A4})$$

Substituting Eqs. (A2), (A3), and (A4) into Eq. (A1), we obtain

$$R_{1s} \frac{d^2(\delta \rho)}{dr^2} + 2 \frac{dR_{1s}}{dr} \frac{d(\delta \rho)}{dr} + 2 \frac{R_{1s}}{r} \frac{d(\delta \rho)}{dr} = [\delta(\mathbf{r}) - \langle \psi_{1s} | \delta(\mathbf{r}) | \psi_{1s} \rangle] R_{1s}. \quad (\text{A5})$$

Define

$$F = d(\delta \rho)/dr. \quad (\text{A6})$$

Equation (A5) reduces to

$$R_{1s} \frac{dF}{dr} + 2 \frac{dR_{1s}}{dr} F + 2 \frac{R_{1s}}{r} F = [\delta(\mathbf{r}) - \langle \psi_{1s} | \delta(\mathbf{r}) | \psi_{1s} \rangle] R_{1s}. \quad (\text{A7})$$

An integrating factor for Eq. (A7) is $r^2 R_{1s}$ (applicable

only when R_{1s} has no node), after applying this, we obtain

$$G(r) = r^2 R_{1s}^2 F = \int_{\infty}^r \frac{R_{1s}^2}{4\pi} \delta(r) dr - \langle \psi_{1s} | \delta(r) | \psi_{1s} \rangle \times \int_{\infty}^r r^2 R_{1s}^2 dr + G(\infty). \quad (\text{A8})$$

Since we have boundary conditions that the wave function and its derivative go to zero at infinity, we then have $G(\infty) = 0$. Also from Eq. (A8) we see that $G(0) = G(\infty) = 0$. Equation (A8) therefore becomes

$$r^2 R_{1s}^2 F = - \langle \psi_{1s} | \delta(r) | \psi_{1s} \rangle \int_{\infty}^r r^2 R_{1s}^2 dr. \quad (\text{A9})$$

Using Eq. (A2), we obtain

$$F(r) = - \frac{\langle \psi_{1s} | \delta(r) | \psi_{1s} \rangle}{P_{1s}^2(r)} \int_{\infty}^r P_{1s}^2(r) dr \quad (\text{A10})$$

and

$$\delta\rho(r) = \int_{\infty}^r F(r) dr + \delta\rho(\infty), \quad (\text{A11})$$

where $\delta\rho(\infty)$ is determined from the condition

$$\langle \delta\phi_{1s,N} | \psi_{1s} \rangle = 0.$$

Doing so, we found

$$\delta\rho(\infty) = \int_{\infty}^0 P_{1s}^2(r) dr \int_{\infty}^r F(r) dr. \quad (\text{A12})$$

Making use of Eqs. (A11) and (A12), Eq. (A4) becomes

$$\delta P_{1s,N} = P_{1s} \left\{ \int_{\infty}^r F(r) dr + \int_{\infty}^0 P_{1s}^2(r) dr \int_{\infty}^r F(r) dr \right\}. \quad (\text{A13})$$

From Eq. (A3), the expression for $\delta\phi_{1s,N}$ is then

$$\delta\phi_{1s,N} = \frac{1}{\sqrt{4\pi}} \frac{P_{1s}}{r} \left\{ \int_{\infty}^r F(r) dr + \int_{\infty}^0 P_{1s}^2(r) dr \int_{\infty}^r F(r) dr \right\}, \quad (\text{A14})$$

where $F(r)$ is given as in Eq. (A10).

Thermal Resistivity at Pb-Cu and Sn-Cu Interfaces between 1.3 and 2.1°K*

L. J. BARNES† AND J. R. DILLINGER

University of Wisconsin, Madison, Wisconsin

(Received 27 July 1965)

Measurements have been made of the thermal resistivity at lead-copper and tin-copper interfaces for $1.3 \leq T \leq 2.1^\circ\text{K}$. By the application of a magnetic field the lead or the tin could be transformed from the superconducting to the normal state. This permitted measurements of the changes in the thermal resistivity at the interface between two metals produced by allowing one of the metals to become superconducting. The thermal resistivity at an interface formed by vacuum casting lead onto copper was found to be $9.3 T^{-3.7} \text{ }^\circ\text{K cm}^2/\text{W}$ with the lead superconducting. An interface formed by growing a single crystal of lead onto a single crystal of copper had an interface resistivity of $9.3 T^{-4.3} \text{ }^\circ\text{K cm}^2/\text{W}$ with the lead superconducting. Upon application of a magnetic field to make the lead normal, the thermal resistivity at the interface dropped to a value too small to measure reliably, less than $0.04^\circ\text{K cm}^2/\text{W}$. These measurements suggest that the heat transfer across Pb-Cu interfaces by electrons is increased considerably by changing the lead from the superconducting to the normal state. The thermal resistivity at the interface between tin and copper, with the tin superconducting, was about $\frac{1}{3}$ as great as that for lead and copper, with the lead superconducting. An alloy zone formed at tin-copper interfaces obscures to some extent the nature of the resistivity at these interfaces. However, heat transfer at Sn-Cu interfaces appears to be dominated by electrons with the tin either superconducting or normal. Heat transfer by electrons at all interfaces behaves qualitatively in a manner similar to the thermal conduction by electrons in the superconductor used. A rod made of alternate layers of Pb and Cu had a much larger thermal resistivity with the lead superconducting than with it normal. This suggests the use of such a sandwich structure as a thermal switch.

INTRODUCTION

THE thermal resistivity ρ at the interface between two different media is defined as the temperature discontinuity ΔT assumed to exist at the interface,

* Work supported by the U. S. Atomic Energy Commission and the Wisconsin Alumni Research Foundation.

† Present address: Atomics International Division of North American Aviation, Inc., Canoga Park, California.

divided by the rate at which heat is transferred across the interface per unit area. This paper presents results of an experimental investigation for $1.3 \leq T \leq 2.1^\circ\text{K}$ of the thermal resistivities at interfaces between lead and copper, and between tin and copper. Since application of a magnetic field could transform the lead or tin from the superconducting to the normal state, it was possible to obtain information concerning the con-